paratively small P–Ti–P angle. Presumably this effect also brings about steric interactions between the phosphide substituents, which accounts for the slight lengthening of Ti–P in **4b** compared to those in **3b**. Such stereochemical influences of unpaired electrons on the geometries of early metallocene dithiolates have been recently examined by Darensbourg et al.[34] As was observed for **3b**, the geometries about the phosphorus atoms in **4b** are pseudotetrahedral. This is marked contrast to that observed for $Cp_2Hf(PEt_2)_2$[17] and $Cp_2Hf(P(SiMe_3)_2)_2$,[32] where one of the two phosphido groups is flattened allowing significant Hf–P π-bonding.

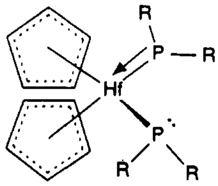

The absence of such interaction in **4b** is yet another ramification of the presence of the singly occupied $1a_1$ orbital.

Summary. The earlier proposals[12,15,21-23] of the mechanism of the formation of the dimer species $[Cp_2Ti(\mu\text{-}PR_2)]_2$ (**2**) involved an initial step of nucleophilic substitution of phosphide for halide followed by rapid reduction to **1** (Scheme I). Dimerization of this species would afford **2**, while reaction with excess phosphide yields **4**. Our results are consistent with this view. The isolation and structural characterization of **3b** and **4b** support the notion of intermediacy of the mononuclear phosphido species **2**. Further the isolation of these species suggests that while the kinetic products of the reaction of Cp_2TiCl_2 and phosphide are mononuclear species, it is the attainment of equilibrium that yields the thermodynamic product, i.e. the dimer **2**.

Acknowledgment. Financial support from the NSERC of Canada is gratefully acknowledged. D.G.D. is grateful for the award of an NSERC of Canada postgraduate scholarship. Dr. R. T. Baker is thanked for helpful discussions regarding the EPR data and communication of structural results prior to publication.

Supplementary Material Available: Tables S1–S3 and S5–S7, listing thermal and hydrogen atom parameters and bond distances and angles (11 pages); Tables S4 and S8, listing values of $10F_o$ and $10F_c$ (14 pages). Ordering information is given on any current masthead page.

Potential Energy Surfaces for Methyl Migration in Tetracarbonylmethylcobalt(I) and Dicarbonylcyclopentadienylmethyliron(II)

Jimmy R. Rogers, Ojin Kwon, and Dennis S. Marynick*

Department of Chemistry, University of Texas at Arlington, Arlington, Texas 76019

Received December 28, 1990

Molecular orbital calculations were used to explore the potential energy surfaces in the methyl migration/carbonyl insertion reactions of tetracarbonylmethylcobalt(I)

$$(CO)_4CoCH_3 \rightarrow (CO)_3Co(COCH_3) \qquad (1)$$

and dicarbonylcyclopentadienylmethyliron(II)

$$CpFe(CO)_2CH_3 \rightarrow CpFe(CO)(COCH_3) \qquad (2)$$

Geometries were determined by using a fast but relatively accurate approximate method (PRDDO), coupled with the synchronous transit approach for estimating transition states. Ab initio calculations using significantly larger basis sets were then used to determine the energetics. In both cases we found low energy barriers to methyl migration as well as small ΔE's for the above reactions. The products of the above reactions, which are the coordinatively unsaturated intermediates in the overall carbonylation reactions, possess minimum energy conformations corresponding to both η^1- and η^2-bound acyl groups. Energetics for the addition of carbonyl will also be presented, as will substituent effects. The results are compared to our previous work involving pentacarbonylmethylmanganese(I), and we contrast these results with recent density functional calculations for the cobalt system.

Introduction

Group migration reactions such as

$$L_nXM\text{-}Y \rightarrow L_nM\text{-}Y\text{-}X$$

play an important role in organometallic chemistry because of their known involvement in homogeneous and heterogeneous catalysis and organic synthesis.[1,2] Group migration in pentacarbonylmethylmanganese(I), for example, has been particularly well-studied. Experimental evidence indicates that the mechanism of this reaction involves the intramolecular migration of the methyl group from the manganese atom to the neighboring carbonyl ligand.[3] This mechanism has been experimentally confirmed in carbonylation reactions using isotopically labeled ^{13}CO, where the labeled ^{13}C does not appear in the acyl position.[4,5] Furthermore, it has been shown that the methyl group in this reaction migrates to a carbonyl ligand cis to the

---

(1) Collman, J. P.; Hegedus, L. S.; Norton, J. R.; Finke, R. G. *Principles and Applications of Organotransition Metal Chemistry*; University Science Books: Mill Valley, CA, 1987; Chapter 6.

(2) Heck, R. F.; Breslow, D. S. *J. Am. Chem. Soc.* **1961**, *83*, 4023.

(3) Calderazzo, F. *Angew. Chem., Int. Ed. Engl.* **1977**, *16*, 299.

(4) Flood, T. C.; Jensen, J. E.; Statler, J. A. *J. Am. Chem. Soc.* **1981**, *103*, 4410.

(5) Noack, K.; Calderazzo, F. *J. Organomet. Chem.* **1967**, *10*, 101.

0276-7333/91/2310-2816$02.50/0

methyl, and the incoming ligand (CO in the case of carbonylation) occupies the vacant site of coordination.[4,5]

In view of its importance, it is not surprising to find that there have been a number of theoretical studies of alkyl migration in transition-metal complexes. Morokuma's group has studied the potential energy surface in the methyl migration/carbonyl insertion reaction of the Pt system:[6]

$$Pt(CH_3)(F)(CO)(PH_3) \rightarrow Pt(COCH_3)(F)(PH_3)$$

Using the (H_3C)–Pt–(CO) angle as the reaction coordinate, this work explored the question of whether the above reaction proceeds via carbonyl insertion into the M–R bond or alkyl migration toward the carbonyl. The calculated potential energy surfaces indicated that the actual mechanism involved is methyl migration. Carbonyl insertion was found to be unlikely due to a very high barrier, whereas a barrier of 22 kcal/mol at the MP2 level was calculated for methyl migration. The methyl migration mechanism was accounted for in this manner: carbonyl insertion is inhibited by the repulsion between the d electrons and the carbonyl lone pair; however, the repulsion between the d electrons and the migrating methyl sp^3 hybrid is small for methyl migration. On this basis, Morokuma and co-workers suggested that carbonyl insertion may be the mechanism involved in early-transition-metal complexes in which d electrons are not abundant. These investigators did not, however, consider an η^2-bound acyl group as a stable conformation of the intermediate, even though its presence is ubiquitous in a number of similar systems. Similar ab initio molecular orbital studies were performed on a palladium complex.[6c,d]

Another system that has been studied theoretically is pentacarbonylalkylmanganese(I). Theoretical work on the migratory-insertion mechanism in $RMn(CO)_5$ has utilized a number of techniques, including extended Hückel theory (EHT)[7] and Hartree–Fock–Slater (HFS) density functional theory.[8] In our laboratory we have previously studied methyl migration in this system[9c,f] by using a combination of partial retention of diatomic differential overlap (PRDDO) and ab initio theory. While details of this study have been presented elsewhere,[9c,f] a brief summary is included here. Ab initio calculations for the closed-shell migration of the methyl group predicted a 17 kcal/mol barrier, while the overall exothermicity of the carbonylation reaction

$$(CO)_5MnCH_3 \xrightarrow{CO} (CO)_5Mn(COCH_3)$$

was calculated to be −8 kcal/mol. Furthermore, the transition-state valence structure for the methyl migration was found to be very acyl-like in nature. This acyl-like character is demonstrated by a C(methyl)–C(acyl) bond length of 1.57 Å, which is quite close to a fully formed C–C bond length of 1.54 Å. In addition, a stable η^2 conformation of the product of migration was predicted. Ziegler's HFS study[8] on the manganese system yielded similar results to our own, with similar ΔE's and a stable η^2-bound acyl species. However, Ziegler and co-workers assumed certain geometrical parameters and did not attempt to locate a transition state.

Finally, methyl migration in $Co(CO)_4CH_3$ has been studied with EHT[7] and HFS density functional theory.[10] With the exception of the work of Morokuma and co-workers[6] and our own previous work on the manganese system,[9c,f] there has been little attempt to characterize the transition states for these systems, and in fact there have been no ab initio studies exploring the entire potential energy surfaces for these species. Due to the importance of these reactions, there exists a clear need for the systematic study of these systems using modern theoretical techniques.

This study extends our previous work on group migration reactions by focusing on the potential energy surfaces for methyl migration in two different transition-metal complexes: tetracarbonylmethylcobalt(I) (reaction 1) and dicarbonylcyclopentadienylmethyliron(II) (reaction 2).

$$(CO)_4CoCH_3 \rightarrow (CO)_3Co(COCH_3) \qquad (1)$$

$$CpFe(CO)_2CH_3 \rightarrow CpFe(CO)(COCH_3) \qquad (2)$$

The cobalt system is particularly important because of its role in hydroformylation reactions.[11] Because the reaction is so facile it has proven difficult to study the cobalt system in full kinetic detail. However, there has been renewed experimental interest in this system due to new methods of probing the kinetics involved.[12,13] Using high-pressure NMR techniques, Roe[12] has found evidence supporting the stabilization of the coordinatively unsaturated intermediate, possibly by acyl oxygen coordination. Sweany[13] used matrix isolation techniques to study the photolysis of $CH_3Co(CO)_4$. He found a similar stabilization of the coordinatively unsaturated acyl complex.

Reaction 2 is another important system to examine. Since the iron reactant and overall product of carbonylation are both tetracoordinate, a number of studies have focused on the mechanism of carbonylation, which can be inferred from stereochemical data available from analogous chiral Fe complexes.[14,15] In the chiral Fe system, methyl migration followed by addition of an external carbonyl should result in inversion of stereochemistry about the metal center. Conversely, if the carbonyl ligand inserts into the $M–CH_3$ bond and the incoming carbonyl occupies the vacant site, then retention of stereochemistry about the metal center is expected. In fact, it is known that both retention and inversion can occur, depending on the solvent, and that both cases are accompanied by some degree of racemization.[15] Furthermore, it is important to note that in the absence of solvent the distinction between intramolecular carbonyl insertion and methyl migration is only meaningful if the intermediate is nonplanar. Since the intermediate is short-lived, its geometry cannot be determined by experimental methods and a theoretical ap-

---

(6) (a) Koga, N.; Morokuma, K. In *Topics in Physical Organometallic Chemistry*; Gielen, M., Ed.; Freund Publishing House Ltd: London, 1989; Vol. 3, Chapter 1. A third mechanism which was described as concerted was also considered. (b) Sakaki, S.; Kitaura, K.; Morokuma, K.; Ohkubo, K. *J. Am. Chem. Soc.* **1983**, *105*, 2280. (c) Koga, N.; Morokuma, K. *J. Am. Chem. Soc.* **1985**, *107*, 7230. (d) Koga, N.; Morokuma, K. *J. Am. Chem. Soc.* **1986**, *108*, 6136.

(7) Berke, H.; Hoffmann, R. *J. Am. Chem. Soc.* **1978**, *100*, 7224.

(8) Ziegler, T.; Versluis, L.; Tschinke, V. *J. Am. Chem. Soc.* **1986**, *108*, 612.

(9) (a) Hansen, L. M.; Marynick, D. S. *Inorg. Chem.* **1990**, *29*, 2482. (b) Hansen, L. M.; Marynick, D. S. *J. Am. Chem. Soc.* **1988**, *110*, 2358. (c) Axe, F. U.; Marynick, D. S. *Organometallics* **1987**, *6*, 572. (d) Jolly, C. A.; Marynick, D. S. *J. Am. Chem. Soc.* **1989**, *111*, 7968. (e) Marynick, D. S.; Axe, F. U.; Hansen, L. M.; Jolly, C. A. In *Topics in Physical Organometallic Chemistry*; Gielen, M., Ed.; Freund Publishing House Ltd: London, 1989; Vol. 3, Chapter 2. (f) Axe, F. U.; Marynick, D. S. *J. Am. Chem. Soc.* **1988**, *110*, 3728.

(10) Versluis, L.; Ziegler, T.; Baerends, E. J.; Ravenek, W. *J. Am. Chem. Soc.* **1989**, *111*, 2018.

(11) Orchin, M. *Acc. Chem. Res.* **1981**, *14*, 259.

(12) Roe, D. C. *Organometallics* **1987**, *6*, 942.

(13) Sweany, R. L. *Organometallics* **1989**, *8*, 175.

(14) Davison, A.; Martinez, N. *J. Organomet. Chem.* **1974**, *74*, C17.

(15) (a) Flood, T. C.; Campbell, K. D. *J. Am. Chem. Soc.* **1984**, *106*, 2853. (b) Forschner, T. C.; Cutler, A. R. *Organometallics* **1985**, *4*, 1247. (c) Hooker, R. H.; Rest, A. J.; Whitwell, I. *J. Organomet. Chem.* **1984**, *266*, C27.

proach such as described here becomes even more desirable. Because there have been a number of experimental studies[15,16] establishing kinetic and thermodynamic properties and the role of the solvent, we will be able to compare our theoretical results with established experimental data.

We present here the first ab initio studies of potential energy surfaces for reactions 1 and 2. Optimized geometries were obtained via the approximate molecular orbital method PRDDO, and the relative energies for these structures were obtained by using ab initio calculations with large basis sets. We estimate the geometries of the transition-state structures from the potential energy surfaces. Substituent effects on the migratory ability of various groups with varying ability to donate or withdraw electron density are also presented. The cobalt and iron systems represented by reactions 1 and 2 will be compared, and our results will be compared with previous results for the manganese system. We will also contrast our results with previous studies, especially with the HFS density functional theory study of the cobalt system,[10] for which we obtain dramatically different results for the structure of the coordinatively unsaturated intermediate.

Calculations

Our approach in examining the potential energy surfaces of these reactions involved using PRDDO to determine geometries, linear synchronous transit (LST) coupled with geometry optimizations to estimate points on the potential energy surface, and large basis set ab initio calculations to determine energetics. PRDDO is an approximate MO method[17] that has been shown[18] to determine the geometries of transition-metal complexes fairly accurately with a substantial savings of computational expense. This coupling of PRDDO with ab initio techniques has worked well in many applications.[9] LST/geometry optimization has been shown to be an efficient way to estimate transition states in these systems, particularly since obtaining transition-state structures with conventional ab initio techniques requires calculating second derivatives. In these large organometallic systems, second-derivative calculations with large basis sets are not feasible in terms of computational time and expense.

In the PRDDO geometry optimizations of the important structures in reactions 1 and 2, standard PRDDO metal basis sets were employed,[18] except for the 3d orbitals, which were derived from atomic optimizations of the ^5D state of Co^+ ($3d^64s^2$) for the cobalt system (reaction 1) and the ^5D state of Fe^{2+} ($3d^44s^2$) for the iron system (reaction 2). The 4s and 4p exponents were set to 2.0. In the geometry optimizations of both systems, all M–C–O angles were fixed at 180°, except for the acyl angles, which were allowed full freedom. All structures in the cobalt system (reaction 1) were additionally constrained to C_s symmetry, while structures in the Fe system (reaction 2) were constrained to fixed C–H and C–O bond lengths at 1.09 and 1.15 Å, respectively. The optimized conformations for the important structures in reactions 1 and 2 are shown in Figures 1 and 2 respectively. A typical single-point energy calculation using PRDDO on an IBM 4381-Q3 computer required 234 s of CPU time or approximately 20 s of CPU time on a Cray X-MP 14/SE system.

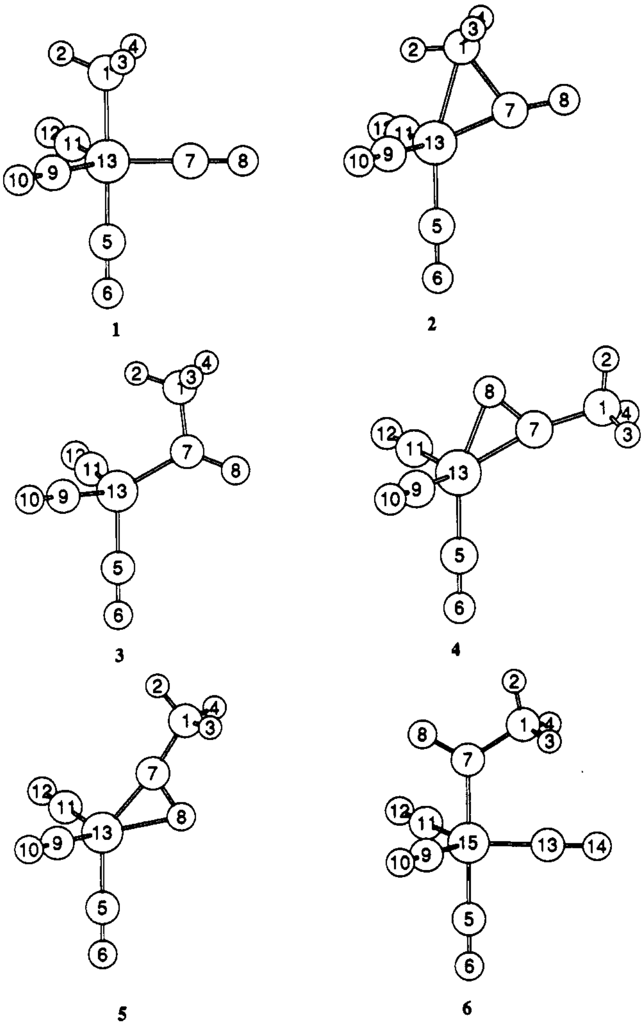

Figure 1. Optimized structures for tetracarbonylmethylcobalt(I). (1) reactant; (2) transition state; (3) intermediate; (4) η^2-A isomer; (5) η^2-B isomer; (6) overall product of carbonylation.

In order to determine the potential energy surfaces for the two reactions, we used the linear synchronous transit approach coupled with geometry optimizations. This approach has proven to work very well in a number of systems, and a fuller description of it is available elsewhere.[19] LST requires that the cartesian coordinates of both reactant and product be placed at "maximum coincidence".[19] As Figure 3 shows, the minimum energy conformation of structures **7** and **9** for the iron system are far from maximum coincidence. However, the Fe–C(acyl) rotation barrier in **9** is very low (5 kcal/mol at the PRDDO level). This is consistent with a recent NMR study of $[(C_6F_5)Ph_2P](CO)(COCH_3)CpFe$, in which the activation barrier for rotation around the $Fe\text{–}COCH_3$ bond was estimated to be 8.5 kcal/mol.[20] Thus the rotation barrier for the Fe–C(acyl) bond is significantly less than the overall barrier to migration (see below). This suggested the following strategy. First, we found the conformation of **9** that minimized its discoincidence index[19] with **7**. This corresponded to rotations of the Fe–C(acyl) and C(acyl)–C(methyl) bonds by 95 and 40°, respectively, and resulted in structure **9′**, which is calculated to be only 4 kcal/mol above **9** at the PRDDO level. This new conformation is shown along with structure **7** in Figure 3. Then we considered the potential energy surface to be divided into two steps: first, **7** → **9′**, and second, relaxation of **9′** into the minimum energy conformation **9**. On the basis of our previous work with $(CO)_5(CH_3)Mn$[9c,f] and Morokuma's work with Pd and Pt systems,[6] we made the simplifying initial assumption that the C(methyl)–M–C(acyl) bond angle varies monotonically along the reaction coordinate. With this approach, the definition of the path coordinate becomes

$$\text{path coordinate} = \frac{\theta_{\text{reactant}} - \theta}{\theta_{\text{reactant}} - \theta_{\text{intermediate}}}$$

where θ = C(methyl)–M–C(acyl). LST calculations were then performed between optimized structures along the surface in order

---

(16) Butler, I. S.; Basolo, F.; Pearson, R. G. *Inorg. Chem.* **1967**, *6*, 2074.

(17) (a) Marynick, D. S.; Lipscomb, W. N. *Proc. Natl. Acad. Sci. U.S.A.* **1982**, *79*, 1341. (b) Halgren, T. A.; Lipscomb, W. N. *J. Chem. Phys.* **1973**, *58*, 1569.

(18) (a) Marynick, D. S.; Axe, F. U.; Kirkpatrick, C. M.; Throckmorton, L. *Chem. Phys. Lett.* **1983**, *99*, 406. (b) Marynick, D. S.; Reid, R. D. *Chem. Phys. Lett.* **1986**, *124*, 17. (c) Marynick, D. S.; Kirkpatrick, C. M. *J. Phys. Chem.* **1983**, *87*, 3273.

(19) Halgren, T. A.; Lipscomb, W. N. *Chem. Phys. Lett.* **1977**, *49*, 225.

(20) Ojima, I.; Kwon, H. B. *J. Am. Chem. Soc.* **1988**, *110*, 5617.

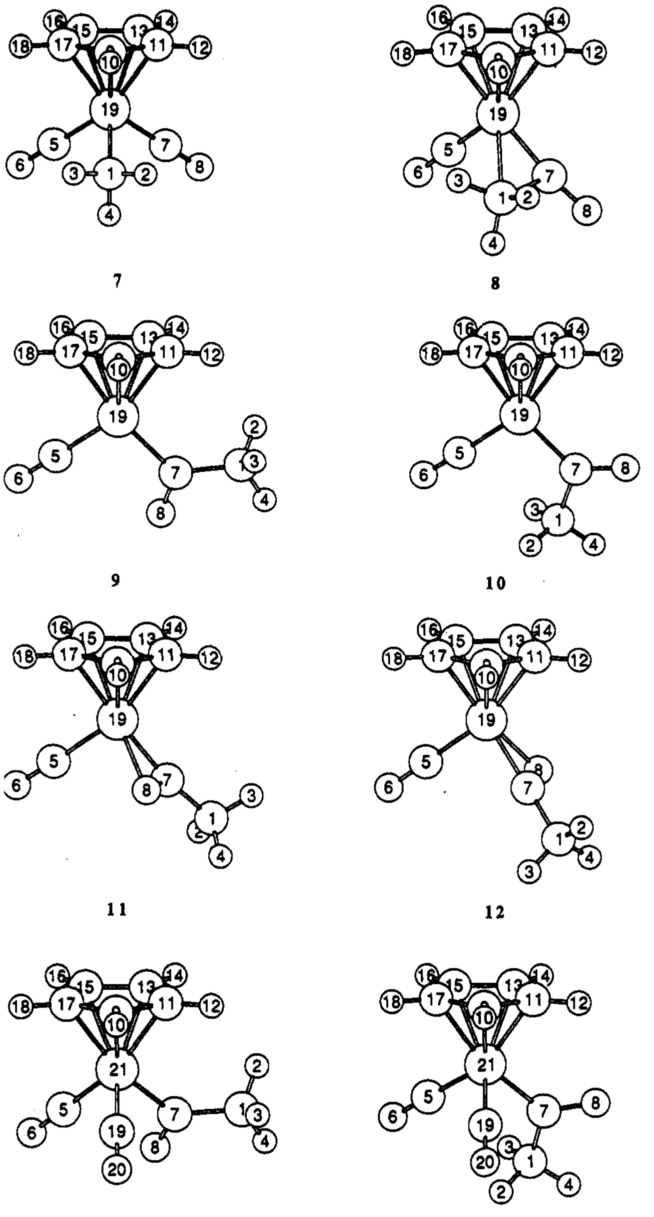

Figure 2. Optimized structures for dicarbonylcyclopentadienylmethyliron(II): (**7**) reactant; (**8**) transition state; (**9**) syn intermediate; (**10**) anti intermediate; (**11**) η^2-A isomer; (**12**) η^2-B isomer; (**13**) syn overall product of carbonylation; (**14**) anti overall product of carbonylation.

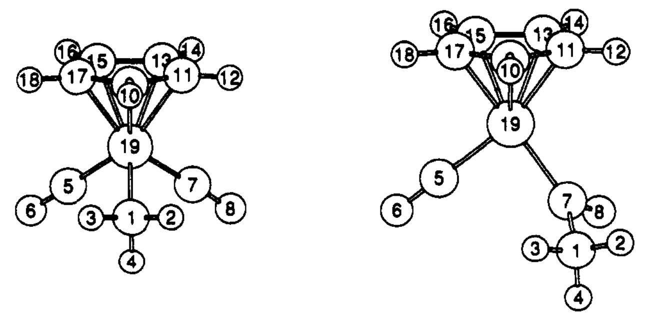

Figure 3. **9'** is obtained from **9** (Figure 2) by rotation about the Fe–C(acyl) bond (see text).

to guarantee an upper bound to the calculated transition-state energy at the PRDDO level. The two potential energy surfaces are shown in Figures 4 and 5.

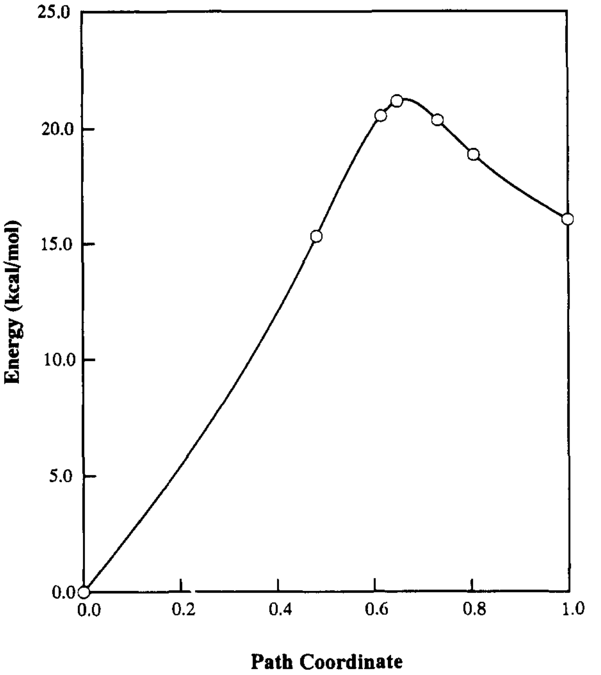

Figure 4. Potential energy surface for methyl migration in tetracarbonylmethylcobalt(I).

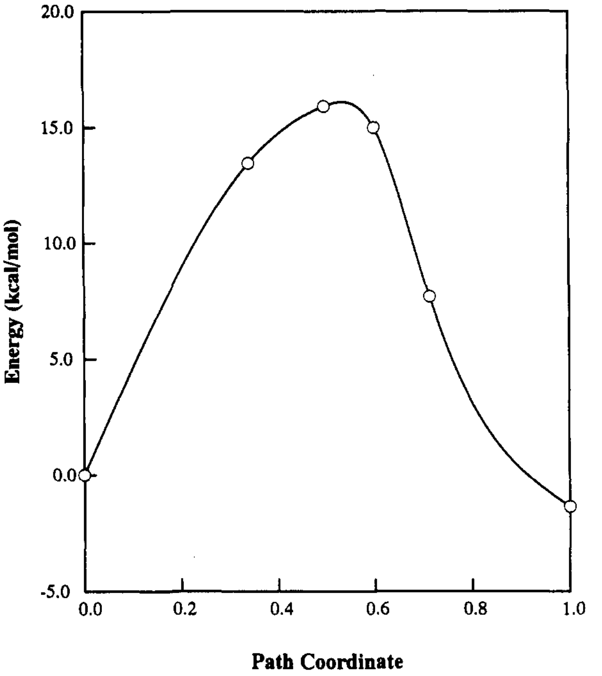

Figure 5. Potential energy surface for methyl migration in dicarbonylcyclopentadienylmethyliron(II).

Ab initio HF calculations were performed by using the GAMESS[21] program. The basis set for the cobalt system (reaction 1) contained 142 basis functions. All of the ligand atoms utilized a 6-31G basis set with the methyl carbon, acyl carbon, and acyl oxygen augmented by six Cartesian d-type polarization functions with values of 0.75 for both carbons and 0.85 for the oxygen. Calculations on the iron system (reaction 2) utilized 143 basis functions with all ligand atoms described by a 4-31G basis set. The basis sets for both metals were minimum basis sets in the core, triple ζ in the 3d/3s space, and double ζ in the 3p, 4s, and 4p regions. Details of the metal basis sets are given in Table I. A typical single-point energy calculation on structures in these systems required approximately 350 min of CPU time on an IBM 4381-Q3 computer.

---

[21] Schmidt, M. W.; Boatz, J. A.; Baldridge, K. K.; Koseki, S.; Gordon, M. S.; Elbert, S. T.; Lam, B. *QCPE Bulletin* **1987**, *7*, 115.

Table I. Orbital Exponents for Cobalt and Iron[a]

	Co	Fe		Co	Fe
1s	26.36220	25.37760	3d	9.329	9.069
2s	9.70545	9.30142	3d′	4.777	4.590
2p	11.54650	11.04470	3d″	2.253	2.174
3p	5.432	5.155	4s, 4p	2.563	2.498
3p′	3.341	3.180	4s′, 4p′	1.539	1.505

[a] These represent Slater orbital exponents. The 1s, 2s, and 2p values were taken from ref 35. The remaining values are from ref 36, basis set A. The valence 4sp exponents were scaled from the atomic values by a factor of 1.47. Gaussian basis sets were generated by taking STO-3G expansions of the 1s, 2s, and 2p orbitals and STO-2G expansions of all other orbitals. See ref 36 for details.

Finally, substituent effects were studied by calculating the activation barriers to migration for two substituents other than methyl at the PRDDO level. These activation barriers were obtained by replacing the methyl substituent with trifluoromethyl or ethyl groups in the PRDDO reactant and transition states. The bond angles of the substituents were then optimized while C_s symmetry was maintained and the geometry of the rest of the molecule was fixed, including the distance between the migratory carbon and the metal atom.

Discussion

1. Tetracarbonylmethylcobalt(I). Table II gives optimized geometries for structures 1–6 depicted in Figure 1, while Table III gives the calculated energies. Figure 4 illustrates the calculated potential energy surface for methyl migration in the cobalt system. Each point on the surface represents a fully optimized PRDDO structure whose energy was subsequently evaluated at the ab initio level. Structure 1 is the reactant in the methyl migration reaction. While the structure of $Co(CO)_4CH_3$ is not known experimentally, our calculated cobalt–carbonyl bond distances (1.82–1.84 Å) agree well with those found experimentally in $Co(CO)_4H$[22] (1.76–1.82 Å) and $Co(CO)_4SiH_3$[23] (1.80 Å).

Structure 2 is the calculated transition state for the migration reaction. In the transition state the C(acyl)–C(methyl) distance has shortened from 2.68 to 1.78 Å, and the Co–C(acyl)–O angle has decreased from 180 to 167.4°. The transition state differs from that previously calculated for pentacarbonylmethylmanganese(I)[9c] in that the latter transition state was found to be much more acyl-like, exhibiting a C(methyl)–C(acyl) bond length of 1.57 Å, practically that of a fully formed C–C bond. The acyl-like nature of the transition state is consistent with thermodynamic information known from other systems.[24,25] The calculated activation energy is 21 kcal/mol, quite similar to that found by using HFS theory (19 kcal/mol).[10]

Three structures are calculated to be stable intermediates in the migration reaction. Structure 3 is the coordinatively unsaturated product of migration. It is higher in energy than the reactant by 16 kcal/mol. The two other structures exhibit the acyl group bound in an η^2 fashion. These η^2 species, structures 4 and 5, are significantly lower in energy than the η^1 intermediate, structure 3. The energies of structures 4 and 5, relative to the reactant, are +3 and −2 kcal/mol, respectively. Thus, η^2 coordination in which electrons from the acyl oxygen occupy the empty site of coordination appears to be important, although our calculations probably overstate the stability of these species. This effective saturation of the cobalt center is corroborated by recent experimental and spectroscopic results.[12,13]

Very significant differences exist between our calculated η^1 intermediate and that found by HFS methods.[10] From a geometrical perspective, our intermediate possesses a relatively normal η^1-bound acyl group, with a C(methyl)–C(acyl) bond distance of 1.55 Å, a C–O distance of 1.23 Å, a C(methyl)–C(acyl)–Co angle of 114.9°, and a Co–C(acyl)–O angle of 129.4°. However the HFS intermediate, with a C–C distance of 1.57 Å, a C–O distance of 1.18 Å, a C(methyl)–C(acyl)–Co angle of 80°, and a Co–C(acyl)–O angle of 150°, actually agrees quite closely with our calculated *transition* state and differs dramatically from our calculated structure for the η^1 intermediate. This is particularly true in terms of the C(methyl)–C(acyl)–Co angle, which is predicted to be 80° in the HFS intermediate and 77.8° in our calculated transition state, and the Co–C(methyl) distance, which is 2.16 Å in the HFS intermediate and 2.24 Å in our calculated transition state. However, it must be pointed out that the C(methyl)–C(acyl) distance in the HFS intermediate is practically a fully formed bond (1.57 Å) and is much closer to that of our intermediate (1.55 Å) than to that of our transition state (1.78 Å).

Analogous intermediates determined by Morokuma and co-workers,[6] namely $Pd(PH_3)(H)COCH_3$ and $Pt(PH_3)(H)COCH_3$, are quite similar to our intermediate and quite different from the HFS intermediate. The calculated intermediate in $Pd(PH_3)(H)COCH_3$ displays a C–C bond distance of 1.58 Å, a C–O distance of 1.21 Å, a C(methyl)–C(acyl)–Pd angle of 101.5°, and a Pd–C(acyl)–O angle of 139.4°. Similarly, the calculated intermediate in $Pt(PH_3)(H)COCH_3$ possesses a C–C bond distance of 1.57 Å, a C–O distance of 1.22 Å, a C(methyl)–C(acyl)–Pt angle of 108.4°, and a Pt–C(acyl)–O angle of 133.4°. Resolution of this discrepancy may require higher level calculations, but we see no reason to doubt the existence of a minimum on the potential energy surface corresponding to an η^1 species with geometrical parameters similar to what we and Morokuma's group have calculated.

Structure 6 represents the overall product of carbonylation, $Co(CO)_4COCH_3$. Its structure is trigonal bipyramidal with the acyl group occupying an axial position. The product of carbonylation is calculated to be more stable than the reactant by 6 kcal/mol. Given the activation barrier to methyl migration of 21 kcal/mol, this indicates an activation barrier for the reverse reaction, the decarbonylation of $Co(CO)_4COCH_3$, of 27 kcal/mol. This compares very well to experimental estimates[12] of a barrier to decarbonylation of 22 kcal/mol.

2. Dicarbonylcyclopentadienylmethyliron(II). Table V gives the optimized geometries for structures 7–14 of the iron system, and these structures are shown graphically in Figure 2. The potential energy surface for methyl migration in this system is depicted in Figure 5. As in the case of the cobalt system above, each point on the surface was fully optimized at the PRDDO level and the energetics were then determined at the ab initio level. Table IV compares our calculated geometry for the reactant, 7, with analogous values from similar compounds and demonstrates that the calculated PRDDO geometry is reasonable. From the perspective of the potential energy surface for migration, the OC–Fe–CO and H_3C–Fe–CO angles are clearly important parameters. Analogous compounds are generally pseudooctahedral,[26] so it is gratifying

---

(22) McNeill, E. A.; Scholer, F. R. *J. Am. Chem. Soc.* **1977**, *99*, 6243.

(23) Robiette, A. G.; Sheldrick, G. M.; Simpson, R. N. F.; Aylett, B. J.; Campbell, J. A. *J. Organomet. Chem.* **1968**, *14*, 279.

(24) Kampmeier, J. A.; Rodehoast, R. M.; Philip, J. B., Jr. *J. Am. Chem. Soc.* **1981**, *103*, 1847.

(25) Blake, D. M.; Winkelman, A.; Chung, Y. L. *Inorg. Chem.* **1975**, *14*, 1326.

(26) (a) Seeman, J. I.; Davies, S. G. *J. Am. Chem. Soc.* **1985**, *107*, 6522. (b) Davies, S. G.; Seeman, J. I. *Tetrahedron Lett.* **1984**, *25*, 1845.

Table II. Geometries for Tetracarbonylmethylcobalt(I)[a]

	reactant 1	transition state 2	intermediate 3	η^2A 4	η^2B 5	carbonylation product 6
Co–C^1	2.00	2.24	2.96	3.40	3.35	3.16
Co–C^7	1.82	1.81	1.95	1.90	1.86	2.04
Co–C^9	1.84	1.84	1.86	1.84	1.85	1.86
Co–C^5	1.82	1.86	1.86	1.86	1.84	1.87
C^1–C^7	2.68	1.78	1.55	1.51	1.51	1.54
C^7–O^8	1.15	1.21	1.23	1.26	1.26	1.23
C^9–O^{10}	1.15	1.15	1.16	1.16	1.15	1.15
C^5–O^6	1.15	1.15	1.15	1.15	1.16	1.15
C^1–Co–C^7	88.9	50.0				
C^1–C^7–Co		77.8	114.9	171.5	168.0	123.4
C^1–Co–C^9	88.4	98.0				
C^7–Co–C^9	122.1	115.5	113.1	104.5	113.5	86.8
C^7–Co–C^5	91.8	113.4	120.7	141.5	120.1	179.6
C^9–Co–C^{11}	115.6	124.3	117.1	115.9	120.8	115.4
C^9–Co–C^5	91.2	89.6	95.5	95.5	93.0	93.0
O^8–C^7–Co	180.0	167.4	129.4	70.2	72.1	120.9

[a] Bond distances in angstroms, bond angles in degrees.

Table III. Relative Energies for Methyl Migration and Carbonylation in $(Co)_4CoCH_3$ (in kcal/mol)

	E_a- (migration)	ΔE- (migration)	ΔE- (carbonylation)
ab initio Hartree–Fock	21	16	−6
Hartree–Fock-Slater[a]	19	17	−5

[a] See ref 10.

Table IV. Geometry[a] of $CpFe(CO)_2CH_3$, Structure 7

	calcd	expt	ref
Fe–C^1	1.96	1.99–2.06	37, 38
Fe–C^5	1.87	1.70–1.83	33, 34, 37, 39–42
Fe–C^9	2.07	1.99–2.26	32–34, 37–39, 42
C^9–C^{11}	1.39		
C^5–O^6	1.15	1.11–1.19	37–42
C^1–Fe–C^5	87.8	88–93.7	26, 23, 38
C^5–Fe–C^7	91.3	90–96	41, 42
O^8–C^7–Fe	180.0	175.6–180	37, 39, 42
C^5–Fe–C^7–O^8	180.0		

[a] Bond distances in angstroms, bond angles in degrees.

to find that our calculated angles of 91.3 and 87.8° are well within the range typically seen for $CpFeL_3$ compounds (Table IV).

The transition-state structure in the methyl migration step, structure 8, occurs earlier in the reaction than the transition states in the analogous cobalt and manganese systems. This is demonstrated by the C(methyl)–C(acyl) bond distance which is 1.82 Å as compared to 1.78 and 1.57 Å in the cobalt and manganese systems, respectively. This is an important bond length to consider, since it gives an indication of how acyl-like the transition state is. This trend of decreasing C–C bond distances in transition states as one proceeds from Fe to Co to Mn can be roughly correlated to M–CH_3 bond strengths, which have been estimated[27] to be 57, 38, and 37 kcal/mol for Fe, Co, and Mn, respectively. Thus it appears likely that as it becomes easier to break the M–CH_3 bond, the transition state occurs later and is more acyl-like in character. In agreement with previous EH results,[7] we find that the stronger M–CH_3 bond present in the iron system results in the migrating methyl group resisting movement from its reactant conformation, while the carbonyl group bends toward the methyl group. Thus, in the transition-state structure, the CH_3 has moved from its previous position by ~14° and the carbonyl has shifted toward the methyl by ~17°.

Surprisingly, however, there is no apparent correlation between M–CH_3 bond strengths and calculated activation energies. The activation energy for methyl migration in dicarbonylcyclopentadienylmethyliron(II) is calculated to be 16 kcal/mol, in good agreement with reported experimental values of 18–26 kcal/mol.[16,28] Furthermore, this calculated activation barrier is similar to our calculated values of 21 and 17 kcal/mol for the cobalt and manganese systems.

Structures 9 and 10 are the unsaturated products of the migration reaction and represent the intermediates in the overall carbonylation. From a mechanistic perspective it is important to note that both intermediates are quasi-trigonal planar rather than pyramidal, as predicted by EHT.[29] This planarity is illustrated by consideration of the important dihedral angles. If the geometrical center of the cyclopentadienyl ring is represented by X, then the dihedral angle formed by the X–Fe–C(acyl) plane with the X–Fe–C(carbonyl) plane is 179.8° for structure 9. Because of this planarity in the isolated intermediate, the structure of the intermediate cannot dictate either retention or inversion of stereochemistry in the final product of carbonylation, and the solvent must play a dominant role in determination of final stereochemistry. This is consistent with the fact that the stereochemistry of carbonylation in optically active CpFe(CO)(L)R is solvent dependent.[15] While our results predicting planarity appear to contradict the EH calculations on a model system,[29] the low barrier to pseudorotation in pentacoordinate species makes this contradiction inconsequential from a stereochemical perspective. Solvent must be invoked to explain *any* systematic retention or inversion of stereochemistry. Nonetheless, it is of considerable interest to examine the differences between the earlier EH conformational analysis[29] and our PRDDO calculated geometry. At the EH level, the HOMO–LUMO gap of the quasi-planar system is very low, and deviations from planarity result in HOMO–LUMO mixing, which increases the HOMO–LUMO gap and stabilizes the pyramidal structure. In contrast, our PRDDO calculations predict a relatively large HOMO–LUMO gap for the planar intermediate (only a 9% reduction from the coordinatively saturated reactant) and a *decrease* in the HOMO–LUMO gap upon distortion to a pyramidal structure.

---

(27) Because PRDDO does not currently have restricted open-shell Hartree–Fock capabilities, which would be required to make reasonable estimates of relative bond dissociation energies, we employed the bond energies calculated in: Ziegler, T.; Tschinke, V.; Becke, A. *J. Am. Chem. Soc.* **1987**, *109*, 1351.

(28) Green, M.; Westlake, D. J. *J. Chem. Soc. A* **1971**, 367.

(29) Hofmann, P. *Angew. Chem., Int. Ed. Engl.* **1977**, *16*, 536.

Table V. Geometries for Dicarbonylcyclopentadienylmethyliron(II)[a]

	7	8	9	10	11	12	13	14
Fe–C^1	1.96	2.14	3.11	3.11	3.37	3.37	3.12	3.11
Fe–C^5	1.87	1.87	1.91	1.90	1.96	1.88	1.92	1.86
Fe–C^7	1.87	1.83	1.99	1.99	1.90	1.89	1.97	1.97
Fe–C^9	2.07	2.05	2.06	2.06	2.07	2.05	2.05	2.06
C^1–C^7	2.66	1.82	1.54	1.54	1.50	1.50	1.53	1.55
C^9–C^{11}	1.39	1.39	1.39	1.39	1.39	1.39	1.39	1.39
C^5–O^6	1.15	1.15	1.15	1.15	1.15	1.15	1.15	1.15
C^7–O^8	1.15	1.18	1.23	1.23	1.26	1.26	1.23	1.23
C^1–Fe–C^5	87.8	88.8	116.7	67.3		90.9	104.5	66.8
C^1–Fe–C^7	87.8	56.6	24.8	24.8			23.6	24.3
C^5–Fe–C^7	91.3	88.0	92.1	93.5	89.0	90.5	80.9	90.6
O^8–C^7–Fe	180.0	178.0	122.0	120.6	70.2	70.2	117.4	120.4
C^1–C^7–Fe		70.0	122.3	122.8	167.2	168.2	125.2	124.3

[a] Bond distances in angstroms, bond angles in degrees.

Table VI. Relative Energies for Methyl Migration and Carbonylation in CpFe(CO)$_2$CH$_3$ (in kcal/mol)

	E_a- (migration)	ΔE- (migration)	ΔE- (carbonylation)
ab initio Hartree–Fock	16	-1	-11
experiment	18,[a] 26[b]		

[a] Reference 28. Measured in acetonitrile. [b] Reference 16. Measured in THF.

Table VII. Substituent Effects: PRDDO-Calculated Activation Barriers for Various Substituents

R	E_a, kcal/mol	R	E_a, kcal/mol
	$Co(CO)_4R \rightarrow Co(CO)_3COR$		
CH$_3$	11.4	C$_2$H$_5$	10.9
CF$_3$	24.1		
	$Cp(CO)_2Fe\text{–}R \rightarrow Cp(CO)Fe(COR)$		
CH$_3$	18.3	C$_2$H$_5$	17.3
CF$_3$	38.5		

The two intermediates **9** and **10** represent the syn and anti conformations, with the primary difference between the two being a 180° rotation of the Fe–C(acyl) bond. The syn conformation is calculated to be 3 kcal/mol more stable than the anti conformation. The overall product of carbonylation exists in two conformations as well, structure **13**, a syn conformation, and structure **14**, an anti conformation. Once again the syn conformation is the more stable conformation, and ab initio calculations predict an overall exothermicity for the carbonylation of dicarbonylcyclopentadienylmethyliron(II) of -11 kcal/mol. This preference for the syn conformation is consistent with ab initio calculations for the model complex CpFe(CO)(PH$_3$)COCH$_3$.[30] However, CpFe(CO)(PPh$_3$)COCH$_3$ and analogous systems are known to be anti[31-34] and preference for this conformation is believed to be due to steric effects.[30]

It is interesting that the ΔE for migration is 17 kcal/mol lower for the iron system relative to that found for CH$_3$Co(CO)$_4$ (compare the energetics in Tables III and VI). A detailed population analysis suggests the following rationale. The migration reaction results in the conversion of an excellent back-bonding ligand (carbonyl) into a poor one (acyl). The intermediate is therefore less stabilized by back-bonding than the reactant. This is of much greater importance in CH$_3$Co(CO)$_4$ than in CpFe(CO)$_2$CH$_3$ since back-bonding effects are much greater for Co$^+$ compared to Fe^{2+}.[43] Thus, Co(CO)$_3$(COCH$_3$) is expected to be destabilized relative to CpFe(CO)(COCH$_3$). However, this effect is not relevant for the overall carbonylation reaction, where the net number of metal–carbonyl bonds remains constant. Accordingly, the ΔE's for the overall carbonylation reactions differ by only 6 kcal/mol.

Structures **11** and **12** represent two stable η^2 conformations of the coordinatively unsaturated intermediate in which the acyl oxygen lone pair is allowed to interact with empty metal d orbitals. Structure **11** is calculated to be more stable than the reactant (**7**) by 5 kcal/mol at the ab initio level, while **12** is more stable than **7** by 2 kcal/mol. While there is at present no direct evidence of stable intermediates in the Fe system that are bound in an η^2 fashion, intermediates such as this are believed to exist in this and similar systems.[1,15a]

3. Substituent Effects. In order to compare the migratory aptitude of organic ligands other than methyl in the cobalt and iron systems, we calculated the activation barriers to migration for two other substituents at the PRDDO level. Results are shown in Table VII. As in our previous study of the manganese system,[9c] we found a tendency for the more electron-withdrawing groups to substantially increase the activation barrier and therefore retard the reaction. Thus, the activation barrier for a trifluoromethyl group was 20 kcal/mol higher than that for methyl in the iron system and was 13 kcal/mol higher than that for methyl in the cobalt system. On the other hand, when an electron-donating group, namely ethyl, was substituted for methyl, the activation barriers were slightly reduced. In the iron system, the ethyl group lowered the activation barrier by 1 kcal/mol, while in the cobalt system, the ethyl group reduced the activation barrier by 0.5 kcal/mol. The underlying reasons for these substituent

---

(30) (a) Davies, S. G.; Seeman, J. I.; Williams, I. H. *Tetrahedron Lett.* **1986**, *27*, 619. (b) Brown, S. L.; Davies, S. G.; Foster, D. F.; Seeman, J. I.; Warner, P. *Tetrahedron Lett.* **1986**, *27*, 623.

(31) Davies, S. G.; Dordor-Hedgecock, I. M.; Sutton, K. H.; Walker, J. C.; Bourne, C.; Jones, R. H.; Prout, K. *J. Chem. Soc., Chem. Commun.* **1986**, 607.

(32) Attig, T. G.; Teller, R. G.; Wu, S. M.; Bau, R.; Wojcicki, A. *J. Am. Chem. Soc.* **1979**, *101*, 619.

(33) Baird, G. J.; Bandy, J. A.; Davies, S. G.; Prout, K. *J. Chem. Soc., Chem. Commun.* **1983**, 1202.

(34) Davies, S. G.; Dordor-Hedgecock, I. M.; Sutton, K. H.; Walker, J. C.; Jones, R. H.; Prout, K. *Tetrahedron* **1986**, *42*, 5123.

(35) Clementi, E.; Roetti, C. *At. Data Nucl. Data Tables* **1974**, *14*, 3.

(36) Hansen, L. M.; Marynick, D. S. *J. Phys. Chem.* **1988**, *92*, 4588.

(37) Ariyaratne, J. K. P.; Bierrum, A. M.; Green, M. L. H.; Ishaq, M.; Prout, C. K.; Swanwick, M. G. *J. Chem. Soc. A* **1969**, 1309.

(38) Brunner, H.; Hammer, B.; Bernal, I.; Draux, M. *Organometallics* **1983**, *2*, 1595.

(39) Batsanov, A. S.; Struchkov, Y. T. *J. Organomet. Chem.* **1984**, *266*, 295.

(40) Kristoff, J. S.; Shriver, D. F. *Inorg. Chem.* **1973**, *12*, 1788.

(41) Gress, M. E.; Jacobson, R. A. *Inorg. Chem.* **1973**, *12*, 1746.

(42) Greene, P. T.; Bryan, R. F. *J. Chem. Soc. A* **1970**, 2261.

(43) Marynick, D. S.; Askari, S.; Nickerson, D. F. *Inorg. Chem.* **1985**, *24*, 868.

Organometallics 1991, *10*, 2823-2827

effects have been discussed in detail previously.[9f]

Conclusion

We have presented the first ab initio HF study of CH_3 migration in tetracarbonylmethylcobalt(I) and dicarbonylcyclopentadienylmethyliron(II). Optimized geometries for important structures on the potential energy surfaces were obtained at the PRDDO level. Energetics were evaluated with large basis set ab initio calculations. At the ab initio level we found activation barriers of 21 kcal/mol for the cobalt system and 16 kcal/mol for the iron system. These values compare well with experimental estimates. The ΔE's for the overall carbonylation reactions were calculated to be -6 and -11 kcal/mol for the cobalt and iron systems, respectively. We examined the potential energy surfaces in order to estimate the transition-state structures, and we found that the transition states were less acyl-like than in the corresponding manganese system. We compared our results with recent HFS calculations on the cobalt system and found that, in general, our energetics are similar. However, our calculated structure for the intermediate (3) differs dramatically from that found previously. Our structure possesses geometrical parameters typical of normal η^1-bound acyl groups,[32-34] while the HFS study found a structure that in fact is very similar to our calculated *transition*-state structure. In contrast to EHT results, we found the structure of the intermediate in the iron system (9) to be quasi-trigonal planar rather than pyramidal. Finally, substituent effects were considered, and our calculations showed that replacing the methyl group with a trifluoromethyl group significantly increases the activation barrier in both systems, while replacing the methyl substituent with an ethyl group slightly reduces the activation barrier.

Acknowledgment. We thank the Robert A. Welch Foundation (Grant No. Y-743), the University of Texas Center for High Performance Computing, and the Texas Advanced Technology Program for their support of this work.

Supplementary Material Available: Cartesian coordinates and total energies of structures 1-14 (13 pages). Ordering information is given on any current masthead page.

Metal-π Complexes of Benzene Derivatives. 37.[1] Redox Behavior of the Sandwich Complexes $C_{12}H_{12}M$ ($C_{12}H_{12}$ = C_6H_6 + C_6H_6, C_5H_5 + C_7H_7; M = V, Cr). A Comparative Study†

Christoph Elschenbroich,* Edgar Bilger, and Bernhard Metz

Fachbereich Chemie der Philipps-Universität, Hans-Meerwein-Strasse, D-3550 Marburg, Germany

Received December 27, 1990

The prototypical sandwich complexes $(\eta^6\text{-}C_6H_6)_2V$ (1), $(\eta^5\text{-}C_5H_5)(\eta^7\text{-}C_7H_7)V$ (2), $(\eta^6\text{-}C_6H_6)_2Cr$ (3), and $(\eta^5\text{-}C_5H_5)(\eta^7\text{-}C_7H_7)Cr$ (4) have been subjected to a cyclovoltammetric study in order to gain insight into the factors that govern the redox processes $C_{12}H_{12}M^{0/-}$ and $C_{12}H_{12}M^{0/+}$. Subsequent oxidation of the cations has also been studied. It is shown that, at constant complex charge, oxidation of the M d^6 species is easier than that of the M d^5 species, and symmetrical complexes (ligands C_6H_6 + C_6H_6) are oxidized preferentially to their unsymmetrical counterparts (ligands C_5H_5 + C_7H_7). The large anodic shift of $E_{1/2}(2^{0/+})$ relative to $E_{1/2}(1^{0/+})$ compared to the small shift of $E_{1/2}(4^{0/+})$ relative to $E_{1/2}(3^{0/+})$ is rationalized on the basis of unequal spin states for 2^+ and 1^+ as opposed to equal spin states for 4^+ and 3^+. The potentials $E_{1/2}$-$(C_{12}H_{12}M^{0/+})$ display an excellent linear correlation with the ionization potentials IP_1 (photoelectron spectroscopy). They also parallel the magnitudes of the appearance potentials (mass spectrometry).

Introduction

Among the four sandwich complexes of general composition $C_{12}H_{12}M$ [$(\eta^6\text{-}C_6H_6)_2V$ (1), $(\eta^5\text{-}C_5H_5)(\eta^7\text{-}C_7H_7)V$ (2), $(\eta^6\text{-}C_6H_6)_2Cr$ (3), and $(\eta^5\text{-}C_5H_5)(\eta^7\text{-}C_7H_7)Cr$ (4)], the redox properties of (cyclopentadienyl)(cycloheptatrienyl)vanadium (2) stand out. This already manifests itself in the rates at which these materials undergo air oxidation, compound 2 being by far the easiest one to handle. In fact, whereas the symmetrical complex 1 in solution is oxidized by air instantaneously, its unsymmetrical counterpart 2 begins to deposit a brown precipitate only after a few minutes and in the solid state is stable in air at room temperature for extended periods of time.[2]

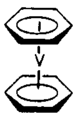

1

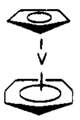

2

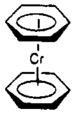

3

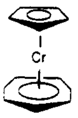

4

This gradation, in particular the contrast between the two isoelectronic complexes 1 and 2, called for an inspection of the ionization potentials for the species $C_{12}H_{12}M$. In this paper, we put data obtained from different methods (cyclic voltammetry (CV), photoelectron spectroscopy (PS), mass spectrometry (MS)) in perspective and offer a rationale for the peculiar behavior of 2, which

---

† Presented at the 200th National Meeting of the American Chemical Society, Symposium on Organometallic Electrochemistry, Washington, D.C., Aug 1990.

(1) Elschenbroich, Ch.; Heck, J.; Massa, W.; Birkhahn, M. *Chem. Ber.* **1990**, *123*, 2321.

(2) King, R. B.; Stone, F. G. A. *J. Am. Chem. Soc.* **1959**, *81*, 5263.

0276-7333/91/2310-2823$02.50/0